Real-time monitoring of the moisture content of filter cakes in vacuum filters by a novel soft sensor

Huttunen Manu, Nygren Lauri, Kinnarinen Teemu, Ekberg Bjarne, Lindh Tuomo, Karvonen Vesa, Ahola Jero, Häkkinen Antti

DOI: 10.1016/j.seppur.2019.03.091

Please cite the publication as follows:

Huttunen M., Nygren L., Kinnarinen T., Ekberg B., Lindh T., Karvonen V., Ahola J., Häkkinen A. (2019). Real-time monitoring of the moisture content of filter cakes in vacuum filters by a novel soft sensor. Separation and Purification Technology, Vol 223. p. 282-291. DOI: 10.1016/j.seppur.2019.03.091

This is an original manuscript of an article published by Elsevier in Separation and Purification Technology on 15 September 2019, available online: https://doi.org/10.1016/j.seppur.2019.03.091.

Real-time monitoring of the moisture content of filter cakes in vacuum filters by a novel soft sensor

Manu Huttunen[a*], Lauri Nygren[a], Teemu Kinnarinen[b], Bjarne Ekberg[b], Tuomo Lindh[a], Vesa Karvonen[b], Jero Ahola[a], Antti Häkkinen[b]

[a]LUT School of Energy Systems, Lappeenranta University of Technology, P.O. Box 20, FI-53851 Lappeenranta, Finland
[b]LUT School of Engineering Science, Lappeenranta University of Technology, P.O. Box 20, FI-53851 Lappeenranta, Finland

[*]Corresponding author: manu.huttunen@lut.fi

Abstract

The moisture content of filter cakes is probably the most important characteristic that should be kept at a desired level in industrial cake filtration applications to maintain consistent product quality and minimize energy consumption. Most of the currently applied methods for contactless real-time monitoring of the moisture content are based for example on x-ray or microwave techniques, and therefore, the equipment for the purpose is highly specialized. This paper introduces a novel soft sensor for filter cake moisture estimation that uses machine learning algorithms and data collected with basic process instrumentation. The method is primarily based on the cooling effect observed in the cake and air, caused by evaporation of liquid from the cake during the dewatering period, and it can be supported by other process data. The specific energy consumption of vacuum filtration and the subsequent thermal drying to zero moisture is also analyzed. The results of pilot-scale experiments with calcite slurry and a horizontal belt vacuum filter show that in order to minimize the specific energy consumption of vacuum filtration, it is crucial to find the right combination of slurry concentration, vacuum level, and mass of filter cake per unit area. The proposed method for estimating the filter cake moisture content is especially suitable for real-time monitoring and control, enabling also considerable reduction in the energy consumption of the overall process. When applying the proposed soft sensor method in a pilot-scale process, the mean absolute error of the estimated moisture content of the filter cake is ~0.4 percentage points when the temperature of air at the vacuum pump inlet and the vacuum pump air flow rate are included in the input variables.

Keywords: Thermodynamics; Vacuum filtration; Dewatering; Moisture content prediction; Soft sensor

This is an original manuscript of an article published by Elsevier in Separation and Purification Technology on 15 September 2019, available online: https://doi.org/10.1016/j.seppur.2019.03.091.

Nomenclature

A	filtration area (m^2)
a	experimentally determined slope t/V^2
c	filtration concentration ($kg/m^3_{filtrate}$)
E	energy consumption (J)
E_S	specific energy consumption (kJ/kg)
L	thickness of the filter cake (mm)
M	moisture content (% kg/kg)
M_s	solids mass flow rate (g/s)
$\dot{m}$	mass flow (kg/s)
m_s	mass of solids (kg)
P	power (W)
p	pressure (bar)
Δp	applied pressure difference (bar)
Q	standard volumetric flow rate (Nm^3/h), heat transfer
q_m	mass flow rate (kg/s)
q_{sl}	slurry mass flow rate (kg/min)
q_V	volumetric flow rate (m^3/s)
R_m	resistance of the filter medium (1/m)
s	solids content (kg/kg)
T	temperature (°C)
ΔT	temperature difference (°C)
t	time (s)
V_f	volume of the filtrate (m^3)
v	velocity (mm/s)
w_a	specific humidity of air (kg_v/kg_a)
w	mass of cake deposited per unit area (kg/m^2)
z	length on filter belt (cm)

Dimensionless number

k	isentropic exponent
R^2	coefficient of determination

Greek symbols

α	specific cake resistance (m/kg)
ε	cake porosity (volume of voids per unit cake volume)
η	efficiency (%)
μ	dynamic viscosity of the filtrate ($N\ s/m^2$)
ρ	density (kg/m^3), Pearson correlation coefficient (-)

Subscripts and superscripts

a	air
av	average
belt	filter belt
c	filter cake
dw	dewatering
e	evaporation
f	filtrate, filtration
in	input value
m	medium
out	output value
S	isentropic, specific
s	solids
sl	slurry
T	isothermal
t	thermal
V	volumetric
v	vapor
vp	vacuum pump
w	water

1. Introduction

Filtration and dewatering operations of easily filtering slurries are commonly performed with vacuum filters, which provide a robust and reliable technology for industrial dewatering. There are several vacuum cake filter designs available, including for instance rotary discs, drum and horizontal belt filters, and table and tilting pan filters [1]. Depending on the filter design, vacuum filters are operated by using different filter media, such as polymeric filter cloths or ceramic filter elements. Most industrial vacuum filters are continuously operating devices with high production

capacities and energy requirements. The importance of vacuum filtration has increased considerably over the past decades [2].

In the cake dewatering stage in vacuum filters, the air flow rate through the cake and the filter medium is high, provided that the applied pressure difference is higher than the capillary threshold pressure of the cake and the filter medium [1,3]. In belt filters equipped with filter cloths there is also a significant ineffective bypass flow at the imperfectly sealed edges of the filter medium. For these reasons, large vacuum pumps consuming considerable amounts of energy are required to maintain the target level of pressure difference. In many vacuum filtration plants, however, the operators typically have no online information about the cake moisture content, nor have the possibility of controlling the rotational speeds of the vacuum pumps to reduce the energy consumption of the process.

The moisture content of the cake at the point of its discharge is one of the most important factors reflecting the filtration and dewatering performance. Determination of the cake moisture content after a dewatering process can be carried out by measuring the weight of a cake sample before and after drying it to complete dryness, according to an appropriate standard (e.g. ASTM D2216). To make it possible to monitor the dewatering process online, without delays caused by the laboratory determination, some indirect methods for the moisture determination have been developed. As an example, the MoistScan® technology by Callidan Instruments, based on a microwave transmission technique, represents an indirect method for online moisture determination in vacuum filters [4]. Other potential methods for the purpose include for instance NMR spectroscopy [5], NIR spectroscopy [6], neutron scattering, and gamma-ray attenuation [7]. Most of these methods have been considered for soil moisture determination, not for continuous filters, where the studied material is in constant movement. On the other hand, theoretical approximation of the cake moisture content is even more challenging because of inevitable variation in the slurry properties and filtration conditions in time, as well as inaccuracy or unavailability of process data. The major factors affecting the filterability have been discussed for example in [8].

The objective of this paper is to introduce a novel soft sensor technique that is suitable for online determination of cake moisture content in industrial vacuum filters. Additionally, the energy consumption of the dewatering stage and the overall material drying process is evaluated.

2. Theory

2.1. Filtration and dewatering of filter cakes

In cake filtration, the solid particles in the slurry are retained on the filter medium during the filtration phase, forming a matrix of solid particles with a void space, i.e., a filter cake. When applying a pressure difference greater than the threshold pressure over the filter cake, air may enter the filter cake and start displacing the liquid. The capillary retention forces holding the liquid in the pores of the filter cake depend on the size range and surface properties of the particles in the cake. For cake filtration, there is also a minimum moisture content, called irreducible saturation, at which the flow of the liquid ceases at any pressure. Increasing the pressure difference over the filter

cake decreases the time required to achieve a certain moisture content or, on the other hand, a lower moisture content is achieved in the same amount of time [9,10].

In the conventional filtration theory, the average specific cake resistance α_{av} is determined from experimental constant pressure filtration data and by using the equation:

$$\frac{t}{V_f} = \frac{\alpha_{av}\mu c}{2A^2\Delta p}V_f + \frac{\mu R_m}{A\Delta p}, \quad (1)$$

where t is time, V_f is the volume of the filtrate, μ is the dynamic viscosity of the filtrate, c is the filtration concentration, i.e., mass of solids collected per volume of the filtrate, A is the filtration area, Δp is the applied pressure difference, and R_m is the resistance of the filter medium [9].

When omitting the resistance of the filter medium and solving Eq. (1) with respect to α_{av}, where a denotes the experimentally determined slope t/V^2, the average specific resistance of the cake is expressed by:

$$\alpha_{av} = \frac{2aA^2\Delta p}{\mu c}. \quad (2)$$

The average cake porosity is the ratio of the void volume of the cake to the total volume of the cake, which can also be calculated by subtracting the solids volume from the total cake volume applying the formula

$$\varepsilon_{av} = 1 - \frac{m_s}{\rho_s AL}, \quad (3)$$

where m_s is the mass of solids, ρ_s is the density of solids, and L is the thickness of the filter cake [10].

In addition to the properties in Eqs. (1)–(3), the mathematical dewatering models derived from the classical filtration theory require the irreducible saturation and threshold pressure of the filter cake as inputs [11]. Furthermore, the assumption underlying the conventional theory is that the specific cake resistance and the porosity are functions of applied pressure only. In reality, the cake porosity and specific resistance depend on time (creep effect) and solids concentration (rate of cake formation) [9,12].

2.2. Thermodynamic background of vacuum dewatering

When considering the thermodynamics of the flow of air through a filter cake with a partially water-saturated void space, the evaporation of water has to be included in the analysis (Fig. 1). The driving force for evaporation of water in the filter cake is the difference of vapor pressures at the saturation and interface temperatures. If the air being forced through the filter cake ($\dot{m}_a$) is

This is an original manuscript of an article published by Elsevier in Separation and Purification Technology on 15 September 2019, available online: https://doi.org/10.1016/j.seppur.2019.03.091.

unsaturated, there will be a difference in vapor pressures. Because of the difference, some of the water will evaporate ($\dot{m}_w$). The latent heat required for this change of state (Q_e) will be drawn from the sensible heat of the water in the cake. As a result, the water will be slightly cooled ($T_w^1 > T_w^2$). The flow of sensible heat from the air and the solids in the filter cake to the water provides the latent heat to evaporate a part of it and a thermal balance is pursued [13].

As a section of the filter cake moves from the start of the dewatering period to the end of the belt, water is both mechanically removed from the filter cake with suction and evaporated. The mechanically removed water is extracted from the process as filtrate, and the evaporated water is extracted in the air evacuated by the vacuum pump. The saturation of the filter cake section decreases as it travels on the filter belt and the flow of air through the filter cake increases. The rates of heat transfer between the liquid and gas phases depend on the properties of the volatile fluid, the dimensions of the interface, and the velocities of flow [13]. Throughout the thickness of the filter cake, heat (Q) is transferred between the liquid water, the cake solids, and the air flowing through. As a result, the filter cake and the air in the vacuum box are at a lower temperature than the room temperature air entering the filter cake ($T_a^1 > T_a^2$). The decreasing saturation and the increasing air flow through the filter cake in the horizontal direction towards the end of the dewatering zone, and the changing temperature through the filter cake in the vertical direction render the phenomena into a multiphase flow and transient heat flow process. For a more detailed account of the governing equations for flow and transport in porous media, the reader is directed to [14].

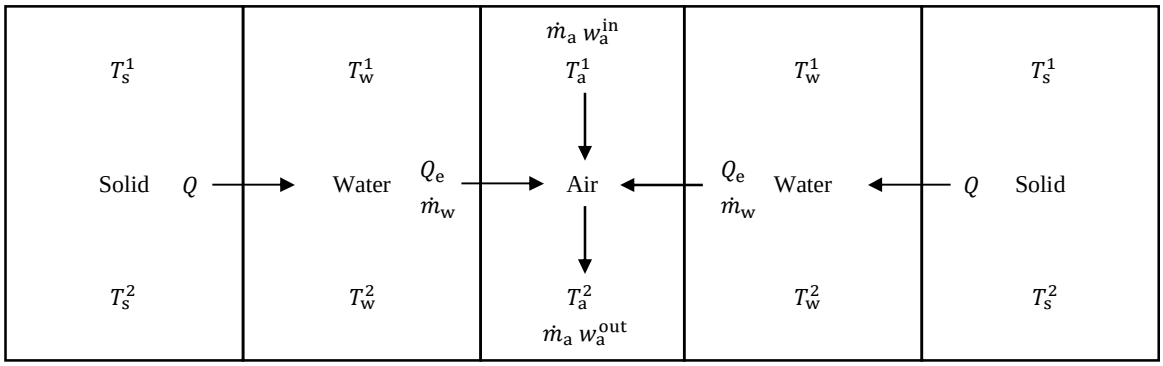

Fig. 1. Diagram illustration of the heat transfer inside the filter cake caused by evaporation. The latent heat Q_e required for evaporation of water will be drawn from the sensible heat of the water. The sensible heat is transferred from the cake solids to the cooled water. In this case $T_x^1 > T_x^2$ and $w_a^{in} < w_a^{out}$.

The mass transfer from water to air by evaporation is proportional to the air mass flow through a filter cake and to the difference between the specific humidity of the outlet and inlet air

$$\dot{m}_w = \dot{m}_a\left(w_a^{out} - w_a^{in}\right), \tag{4}$$

where $\dot{m}$ is the mass flow, the subscripts w and a denote water and air, and w_a is the specific humidity of air [15]. On the other hand, in an air-water vapor mixture, the rate of mass transfer is roughly proportional to the rate of heat transfer at the interface [13].

2.3. Power demand

In vacuum filtration processes, the pressure difference across the filter cake is generated by a vacuum pump. The ideal isentropic power demand P_S of a dry claw vacuum pump for a given inlet volumetric flow rate $q_{V,in}$ generated by the pump can be calculated by the equation

$$P_S = \frac{k}{k-1} q_{V,in} p_{in} \left[\left(\frac{p_{out}}{p_{in}} \right)^{\frac{k-1}{k}} - 1 \right], \quad (5)$$

where p_{in} is the pressure at the inlet of the vacuum pump, p_{out} is the outlet pressure of the vacuum pump, and k is the isentropic exponent. For a cooled vacuum pump, such as a liquid-ring vacuum pump, the isothermal power demand P_T can be used to describe the ideal process,

$$P_T = q_{V,in} p_{in} \ln \left(\frac{p_{out}}{p_{in}} \right). \quad (6)$$

If the moisture content of the product after vacuum filtration is too high, additional drying is required. In thermal drying, the moisture is removed from the cake by evaporation. Ideally, the power P_v required to provide the heat for evaporation can be calculated by using the equation

$$P_v = q_{m,v} \Delta H_v = q_{m,s} \left(\frac{1}{s_{in}} - \frac{1}{s_{out}} \right) \Delta H_v, \quad (7)$$

where q_m is the mass flow, ΔH_v is the latent heat of evaporation, and s_{in} is the weight per weight solids content of the filter cake after vacuum filtration [16]. The subscript v denotes vapor and s solids. For ideal evaporation, it is assumed that all the supplied energy goes to heating of the matter and evaporation of water. The specific heat used in the calculations for water and calcite solids is c_w = 4.186 kJ/(kg K) and c_s = 0.8 kJ/(kg K) respectively, and the latent heat for evaporation of water ΔH_v = 2256 kJ/kg [17].

This is an original manuscript of an article published by Elsevier in Separation and Purification Technology on 15 September 2019, available online: https://doi.org/10.1016/j.seppur.2019.03.091.

3. Materials and methods

3.1. Preparation of slurries

The slurries used for the experiments were prepared from Nordkalk Parfill H80 calcite and tap water to form a variety of slurries with dimensionless weight based solids contents in the range of 0.26–0.44. The particle size distribution of solids was measured with a Malvern Mastersizer 3000 particle size analyzer. Five parallel measurements were performed, and the average distribution (Fig. 2) was then produced by using a software provided by the analyzer manufacturer.

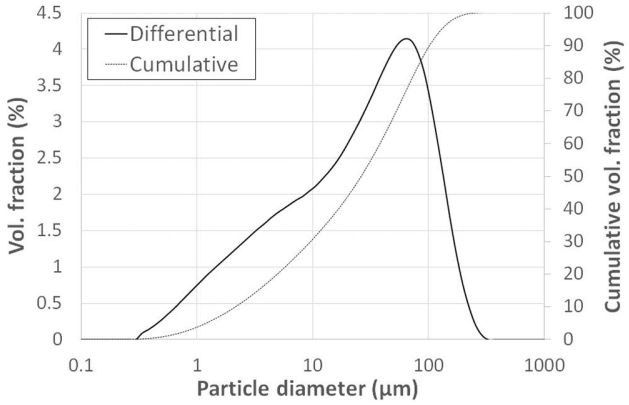

Fig. 2. Particle size distribution of Nordkalk Parfill H80.

3.2. Equipment and instrumentation

Filtration experiments were conducted using a pilot-scale horizontal belt vacuum filter with a reciprocating tray. The main operational parts of the machine comprise slurry infeed, filter belt, vacuum generation by a claw or a liquid-ring vacuum pump, and filtrate handling. The filter belt effective length is 2.1 m and the width is 10 cm. The instrumentation of the device is illustrated in Fig. 3. The majority of the experiments were run with the claw vacuum pump and 16 experiments with the liquid-ring vacuum pump.

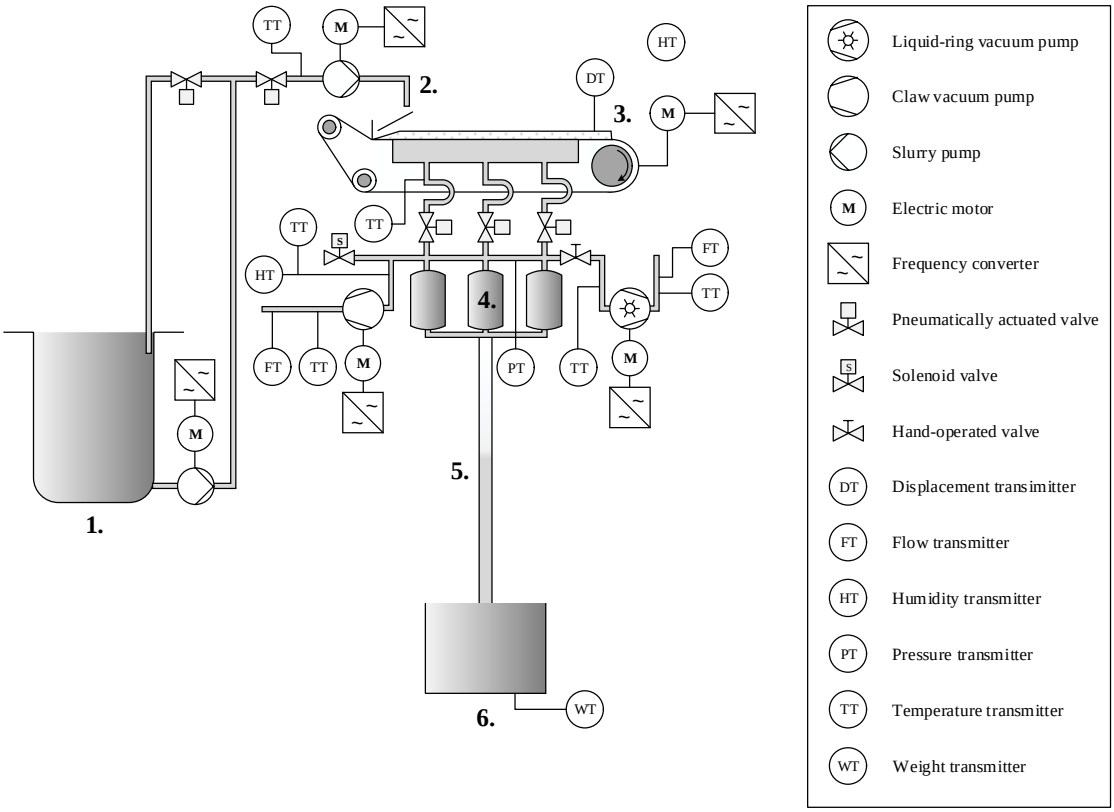

Fig. 3. Horizontal belt vacuum filter device setup and instrumentation: 1) slurry tank, 2) slurry infeed, 3) cake discharge, 4) filtrate intermediate tanks, 5) barometric leg, and 6) filtrate collection tank.

3.3. Experimental work

Experiments were conducted with various weight based slurry solids contents s_{sl} and masses of cake solids deposited per unit area w varying also the pressure difference Δp over the filter cake. The mass of cake deposited per unit area was varied by varying the feed flow rate q_{sl} and the belt speed v_{belt}. The varied experiment settings determined the slurry density ρ_{sl} and the solids mass flow rate M_s. Summary statistics of the experiment settings with mean μ, standard deviation σ, minimum, 25th percentile, median, 75th percentile, and maximum values are presented in Table 1. The subscripts sl, s, and belt denote the slurry, solids, and the filter belt. The complete settings and measurement results for a total of 80 experiments are presented in an [dataset] additional file.

This is an original manuscript of an article published by Elsevier in Separation and Purification Technology on 15 September 2019, available online: https://doi.org/10.1016/j.seppur.2019.03.091.

Table 1. Summary statistics of the settings of a total of 80 experiments. The symbols μ and σ denote mean and standard deviation.

	Δp (bar)	s_{sl} (-)	ρ_{sl} (kg/m^3)	q_{sl} (kg/min)	M_s (g/s)	v_{belt} (mm/s)	w (kg/m^2)
μ	0.34	0.33	1259	1.1	5.8	6.6	9.7
σ	0.11	0.07	69	0.2	0.9	2.3	3.2
min	0.20	0.26	1192	0.6	4.4	5.0	4.4
25 %	0.30	0.28	1214	1.0	5.0	5.0	6.5
50 %	0.31	0.29	1221	1.1	5.8	5.0	10.1
75 %	0.40	0.39	1323	1.2	6.5	10.0	12.1
max	0.61	0.44	1384	1.5	7.4	10.0	14.7

When running the experiments, the filtration process was allowed to stabilize to a steady state, in other words, to a steady filtration length before data collection was started. The pressure difference was held at a constant level using a programmable logic controller (PLC) and a variable speed drive (VSD) for the vacuum pump. The slurry infeed rate and the belt speed were also kept constant during the data collection with the help of variable speed drives. Data were collected from the filter instrumentation using the PLC and a 100 ms sampling rate. For a number of experiments, the surface temperature of the filter cake in the dewatering zone was measured with a PeakTech 4695 infrared thermometer. The device has a measuring range from -50 °C to +380 °C and a distance/spot ratio of 12:1. The measurement distance perpendicular to the filter cake was 10 cm, and the measurements were made along the centerline of the filter cake.

Cake samples were collected from the scraper located at the end of the filter belt to determine their dimensionless weight based solids contents s and the weight based moisture contents percentage M. The cake samples were weighed wet immediately after sampling, dried to zero moisture, and reweighed. The total solids content of each slurry was determined by collecting two parallel samples from the slurry recirculation loop and processed in the same way as the cake samples.

3.4. Regression models

Mathematical models of processes that are designed based on experimental data to estimate relevant process variables are known as inferential models, virtual sensors, or soft sensors [18]. Data-driven methods for building soft sensor models to estimate difficult to measure quality variables of a process have gained much attention in recent years [19–26]. Machine learning algorithms serve as basic tools for constructing models from relationships between difficult to measure quality or key variables and easy to measure variables [27]. Contactless online measurement of the filter cake moisture content requires special equipment that uses for instance x-rays or microwave radiation. A reliable soft sensor model for moisture content could possibly render the use of special equipment and radiation obsolete.

The development of a special soft sensor regression algorithm for the solids content of the filter cake is beyond the scope of this study. The aim of experimenting with machine learning algorithms was to find the simplest model with reliable estimation results. To this end, soft sensor regression was experimented with five standard machine-learning algorithms, namely regularized linear regression algorithms Lasso, Ridge, and Elastic-Net as well as ensemble decision tree algorithms

Random Forest and Gradient Boosting capable of modeling non-linear relationships between variables.

The data set was randomly divided into training and testing sets with 80% and 20% of data respectively. The models were trained with fivefold cross-validation using algorithms provided in the Scikit-Learn software package. For hyperparameter tuning, the strengths of penalty for Lasso, Ridge, and Elastic-Nets were 0.001, 0.005, 0.01, 0.05, 0.1, 0.5, 1, 5, and 10, and for Elastic-Net the L_1-ratios were 0.1, 0.3, 0.5, 0.7, and 0.9. The number of estimators for the decision tree algorithms were 10, 20, 40, 60, 80, 100, and 200. The tuned maximum features settings for the Random Forest Algorithm were auto, sqrt, and 0.33. The Gradient Boosting tuned learning rates were 0.05, 0.1, and 0.2, and the maximum depths 1, 3, and 5.

4. Results and discussion

4.1. Summary statistics of filtration results

The pressure difference range for the experiments was from 0.2 to 0.6 bar, and the mass of solids per unit area on the filter belt varied between 4.4 and 14.7 kg/m^2. This resulted in a filter cake height L_c varying between 2.1 and 8.0 mm. Experiments with extremely short and long filtration lengths z_f were also ran for values between 30 and 190 cm. The mean moisture content of the filter cakes M was 16.6 % with a standard deviation of 1.3 percentage points (pp). Summary statistics of filter cake properties are presented in Table 2. The subscripts f, dw, c, and av denote filtration, dewatering, filter cake, and average. Filtration results for all the 80 experiments are presented in an [dataset] additional file.

Table 2. Summary statistics of filter cake properties for a total of 80 experiments. The symbols μ and σ denote mean and standard deviation. For other symbol definitions, see Nomenclature.

	Δp (bar)	w (kg/m^2)	z_f (cm)	t_f (s)	t_{dw} (s)	L_c (mm)	ε_{av} (-)	s (-)	M (%)
μ	0.34	9.7	110	189	162	5.2	0.34	0.834	16.6
σ	0.11	3.2	35	85	63	1.7	0.08	0.013	1.3
min	0.20	4.4	30	30	30	2.1	0.04	0.797	14.7
25 %	0.30	6.5	94	115	118	3.9	0.28	0.829	15.7
50 %	0.31	10.1	110	199	160	5.6	0.35	0.836	16.4
75 %	0.40	12.1	130	249	209	6.6	0.40	0.843	17.1
max	0.61	14.7	190	379	349	8.0	0.46	0.853	20.3

4.2. Volumetric air flow rates

During the dewatering phase, air flows through the partly desaturated porous filter cake. As can be seen on the left in Fig. 4, the air flow rate increases with an increasing pressure difference and length of the dewatering zone. The results show that within a similar pressure difference range, i.e., the pressure differences 0.2, 0.3, 0.4, and 0.5 bar, an overall increasing trend in the air flow rate with the increasing dewatering zone length is observable. There are, however, exceptions to this trend, and smaller slurry loading and thereby a longer dewatering zone length does not mean a

higher air flow rate in all cases. This is interesting in the sense that with a thinner filter cake one might expect to get more leak flow at the edges of the filter cake.

As more air is pumped through the vacuum pump and the filter cake, the temperature difference between the vacuum pump inlet air and the slurry feed increases (Fig. 4 on the right). This would indicate a higher heat transfer rate between water and air and thereby a greater evaporation rate.

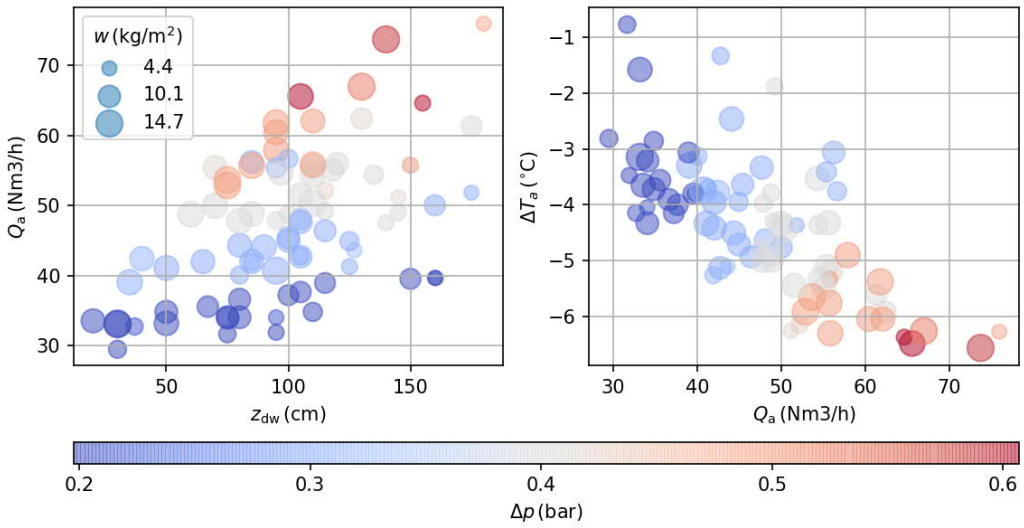

Fig. 4. Air flow rates through the vacuum pump Q_a plotted against the dewatering length z_{dw} (left) and the temperature difference between the vacuum pump suction air and the slurry feed ΔT_a plotted against the air flow through the vacuum pump Q_a (right). The size of the marker is varied according to the mass of cake deposited per unit area w and the color according to the pressure difference Δp.

4.3. Solids contents of filter cakes

The filter cake solids content after dewatering s_c with respect to the dewatering time is depicted on the left in Fig. 5. In general, a higher solids content is achieved with a higher pressure difference and a longer dewatering time. The correlation of the filter cake solids content with the pressure difference and the dewatering time arouses interest to study how the interaction feature of the pressure difference and the dewatering time correlates with the solids content. As can be seen on the right in Fig. 5, the product of these two features yields a stronger correlation with the filter cake solids content.

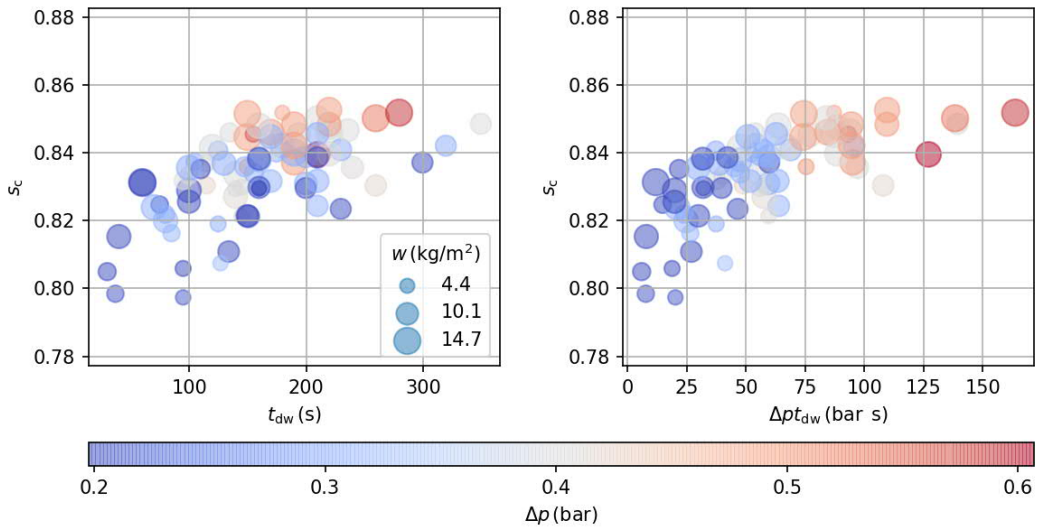

Fig. 5. Filter cake solids content plotted against the dewatering time t_{dw} (left) and the pressure difference multiplied by the dewatering time Δpt_{dw} (right). The size of the marker is varied according to the mass of cake deposited per unit area w and the color according to the pressure difference Δp.

As expected, a higher pressure difference and a higher vacuum pump air flow rate, maintaining that pressure difference, yields a drier cake as can be seen as a general trend on the left in Fig. 6. A lower air temperature measured at the vacuum pump inlet would suggest a drier cake as illustrated on the right in Fig. 6. As the air entering the filter cake was at a room temperature, the deviation in that temperature is small and thus neglected in this study. The correlation between the solids content of the cake and the air temperature at the vacuum pump inlet is in line with the thermodynamic background of vacuum dewatering described in the theory section.

This is an original manuscript of an article published by Elsevier in Separation and Purification Technology on 15 September 2019, available online: https://doi.org/10.1016/j.seppur.2019.03.091.

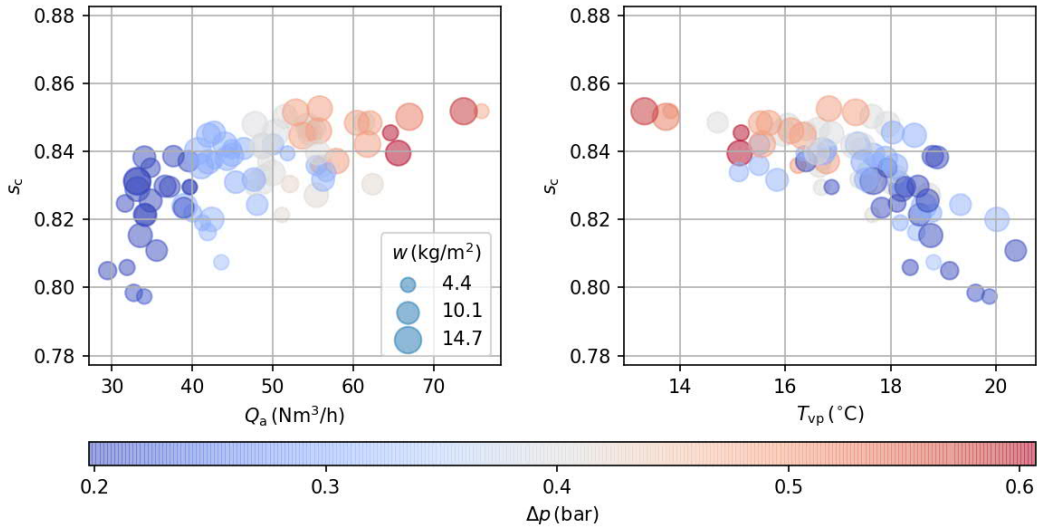

Fig. 6. Filter cake solids content plotted against air flow rates through the vacuum pump Q_a (left) and air temperature at the vacuum pump inlet T_{vp} (right). The size of the marker is varied according to the mass of cake deposited per unit area w and the color according to the pressure difference Δp.

In most cases, a greater temperature difference between the vacuum pump suction air and the slurry feed seems to indicate a drier cake as can be seen in Fig. 7. Variations in the interdependence of these two features could be caused for example by the increased leak flow around the edges of the filter cake that would make the air mixture at the vacuum inlet warmer.

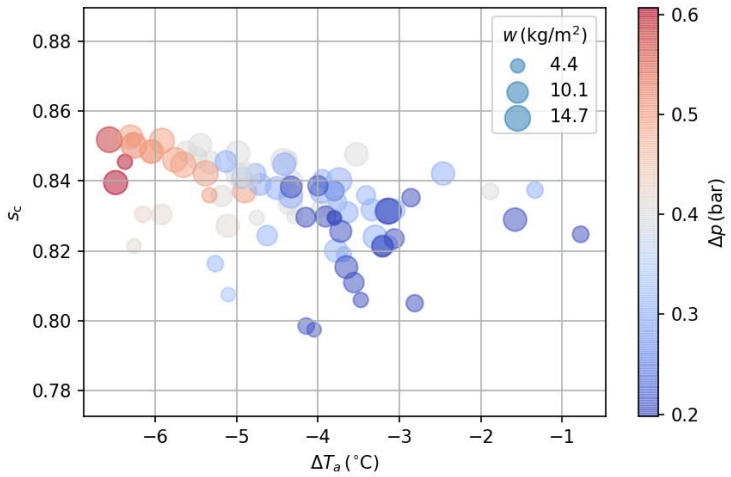

Fig. 7. Filter cake solids content plotted against temperature difference between the vacuum pump suction air and the slurry feed. The size of the marker is varied according to the mass of cake deposited per unit area w and the color according to the pressure difference Δp.

For a limited number of experiments, the surface temperature of the filter cake in the dewatering region was measured, and the minimum, mean, and maximum values for each vacuum level are depicted in Fig. 8. The slurry solids content for these experiments was held constant, but the slurry infeed and filter belt speed were adjusted to vary the slurry loading on the belt. As more and more water was evaporated from the pore space of the filter cake towards the end of the belt, more and more sensible heat was removed from the cake and the temperature of the filter cake decreased. The slope of the temperature profile suggests that the cooling effect would continue for some time if the filter belt were longer. As can be clearly seen in Fig. 8, the greater the pressure difference over the filter cake is, the greater is the temperature change on the surface of the filter cake.

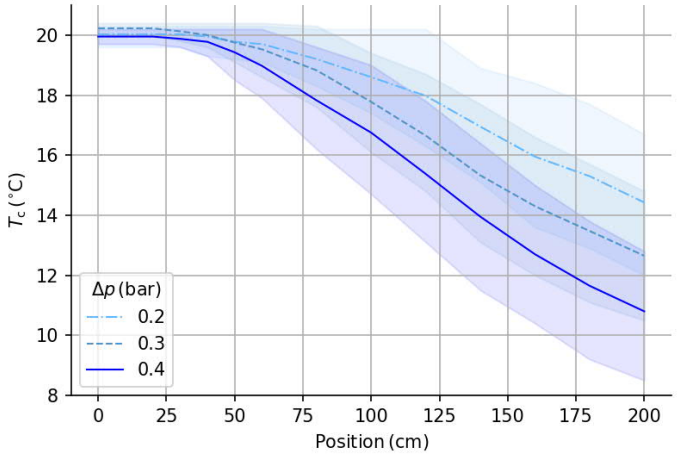

Fig. 8. Mean filter cake surface temperature profiles along the filter belt (lines) and variation between the minimum and maximum temperatures due to varying slurry loadings (filled area) at the corresponding pressure difference levels.

From the limited number of experiments with cake surface temperature measurements, it can be concluded that the change in the cake temperature seems to give an indication of the solids content of the filter cake as depicted in Fig. 9. In general, the greater the pressure difference is, the greater is the temperature change of the filter cake in the dewatering zone and the drier is the filter cake. It was also found that the cake surface temperature varies greatly also in the direction perpendicular to the filter belt movement. Hence, in the future research, it would be a good idea to measure the filter cake temperature along the whole width of the cake.

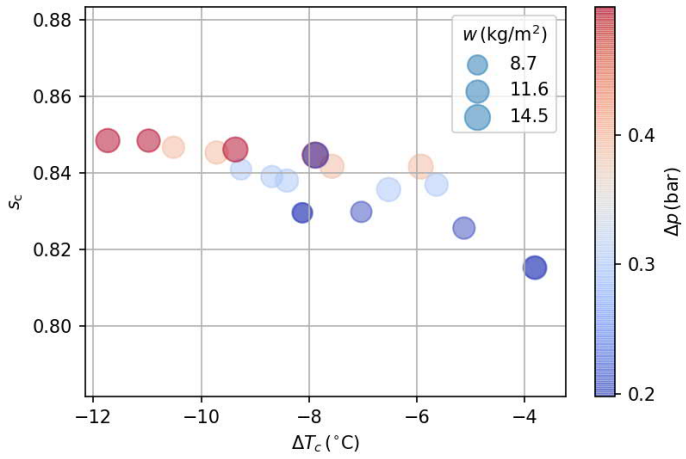

Fig. 9. Filter cake solids content plotted against temperature difference between the filter cake surface at the end of the dewatering region and slurry feed. The size of the marker is varied according to the mass of cake deposited per unit area w and the color according to the pressure difference Δp.

4.4. Specific energy consumption

To investigate the specific energy consumption of vacuum filtration and to minimize the variation in results arising from the two different types of vacuum pumps used in the study, theoretical power demand calculations for the two pumps were made using Eqs. (5)–(6). The power demand of thermal drying of the filtration product to zero moisture was calculated by Eq. (7). The specific energy consumption of vacuum filtration, $E_S^f = E^f/m_s$, versus the filter cake solids content is illustrated in Fig. 10. The specific energy requirement of vacuum filtration increases exponentially as the pressure difference is increased. Similar findings were also observed by the authors of [28] in experiments conducted using a Büchner filter. For experiments with the filter cake solids content between 0.835 and 0.845, the results show nearly a tenfold increase in the specific energy consumption of vacuum filtration from 29.5 to 291 kJ/kg as a result of the increasing pumping demand for maintaining a higher pressure difference. When increasing the solids content of the filter cake from 0.84 to 0.85, the specific energy consumption almost tripled from 56.1 to 153 kJ/kg. For experiments with the pressure difference of 0.2 bar, the solids content varied by 4.1 pp between 0.797 and 0.838 while the specific energy consumption remained below 50 kJ/kg.

This is an original manuscript of an article published by Elsevier in Separation and Purification Technology on 15 September 2019, available online: https://doi.org/10.1016/j.seppur.2019.03.091.

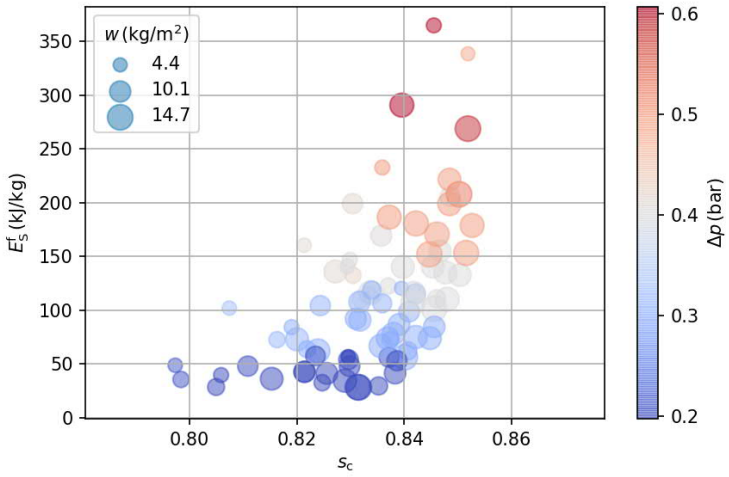

Fig. 10. Specific energy consumption of vacuum filtration plotted against filter cake solids content. The size of the marker is varied according to the mass of cake deposited per unit area w and the color according to the pressure difference Δp.

The theoretical specific energy consumption of thermal drying, $E_S^t = E^t/m_s$, i.e., evaporation of the residual moisture content in the filter cake was calculated with the help of Eq. (7) and assuming a thermal efficiency η=50% of the drying process based on the heat efficiency of a spin-flash dryer reported by Kudra et al. [29]. The specific energy consumption of thermal drying versus the filter cake solids content is depicted on the left in Fig. 11. The moist solids are heated to 100 °C from the initial temperature, which is assumed to be the same as the vacuum pump inlet air temperature. A higher solids content decreases the energy required in the thermal drying stage. The majority of the energy in drying is consumed by the evaporation of water and the small deviations from the decreasing linear energy demand trend are due to the differences in the initial temperature (after dewatering) of the filter cake. The total specific energy consumption to zero moisture, i.e., the sum of the specific energy consumption of vacuum filtration and the specific energy consumption of thermal drying (evaporation), $E_S^{tot} = E_S^f + E_S^t$, versus the filter cake solids content after dewatering, is presented on the right in Fig. 11. The optimum operating conditions in terms of specific energy consumption for the pilot-scale filter and the slurry in question seem to concentrate around the solids content of 0.84, emphasizing the importance of online tracking of the filter cake solids content. Given that the total specific energy consumption mostly varies from 1000 to 1150 kJ/kg, the potential for energy conservation by optimizing slurry concentration, pressure difference, and cake deposited per unit area could be as high as 13 % in this case. In order to identify the optimum operating point, the experiments with the total specific energy consumption in the lowest 10% are presented in Table 3 in an ascending order according to the total specific energy consumption.

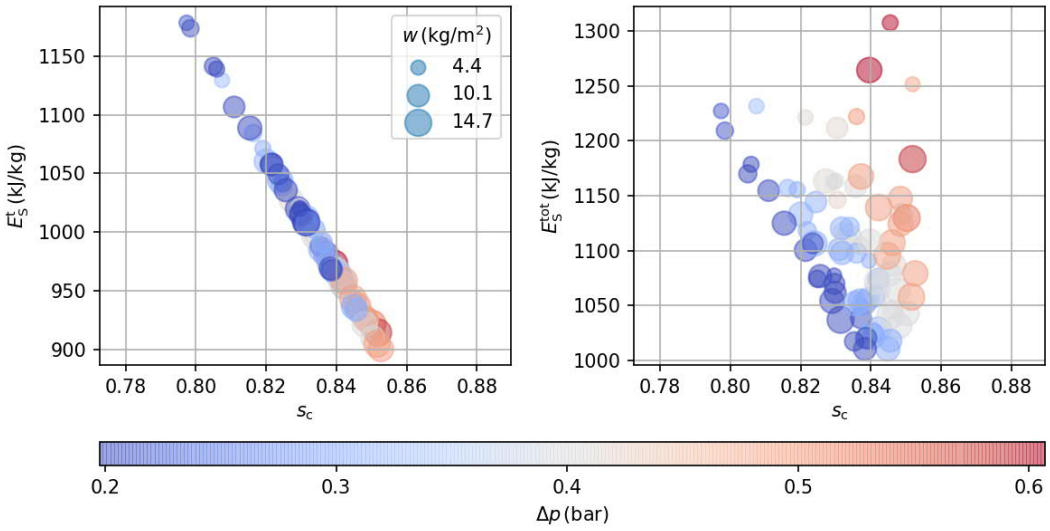

Fig. 11. Specific energy consumption of evaporation of the residual moisture content of the filter cake (left) and the total specific energy consumption to zero moisture (right) plotted against filter cake solids content. The size of the marker is varied according to the mass of cake deposited per unit area w and the color according to the pressure difference Δp.

The total specific energy consumption to zero moisture within the lowest 10 % is achieved with pressure differences ranging from 0.2 to 0.3 bar. All these experiments with the exception of one are from the test series with two of the highest levels of the slurry solids content. The majority of the experiments with a low total specific energy consumption are from experiments with a slow filter belt speed and a high mass of cake deposited per unit area w. The solids contents after vacuum filtration for the experiments in Table 3 is between 0.835 and 0.846. With one exception, the porosities of the experiments are within the 50th percentile, and six of them deviate from the 25th percentile by 3 pp or less. The two minimum energy consumption values are achieved with the slurry solids content of 0.39 and long filtration times, the second-row experiment having an increase in the mass of cake deposited per unit area w and in the pressure difference compared with the first-row experiment. Compared with the two minimum specific energy consumption experiments, increasing the slurry solids content to 0.44 and shortening the filtration time by increasing the filter belt speed, produces a thinner, higher porosity cake with only a 6–7 kJ/kg (0.6–0.7%) increase in the total specific energy consumption but a 25 to 42 % increase in the solids throughput M_s.

This is an original manuscript of an article published by Elsevier in Separation and Purification Technology on 15 September 2019, available online: https://doi.org/10.1016/j.seppur.2019.03.091.

Table 3. Filtration experiments with the total specific energy consumption in the lowest 10%. For symbol definitions, see Nomenclature.

s_{sl} (-)	ρ_{sl} (kg/m^3)	w (kg/m^2)	M_s (g/s)	Δp (bar)	L_c (mm)	z (cm)	t_f (s)	t_{dw} (s)	s (-)	ε_{av}	M (%)	E_S^{tot} (kJ/kg)
0.39	1323	10.4	5.2	0.20	5.1	130	259	160	0.838	0.27	16.2	1010
0.39	1323	11.7	5.9	0.30	5.7	125	249	170	0.845	0.27	15.5	1011
0.44	1384	7.4	7.4	0.20	4.2	100	100	110	0.835	0.36	16.5	1017
0.39	1323	10.4	5.2	0.30	5.0	105	209	209	0.846	0.24	15.4	1018
0.39	1323	9.1	4.6	0.20	4.4	105	209	209	0.839	0.25	16.1	1020
0.44	1384	14.7	7.4	0.30	7.6	115	229	190	0.840	0.31	16.0	1022
0.44	1384	7.4	7.4	0.30	3.9	85	85	125	0.841	0.31	15.9	1025
0.34	1270	12.1	6.1	0.30	5.8	120	239	180	0.842	0.25	15.8	1029

4.5. Prediction of the moisture contents of filter cakes

Nine combinations of experiment settings, measured process values, and interaction features were used as inputs to the regression models (Table 4) to predict the filter cake solids content after dewatering. The correlation map of the correlation coefficients ρ between these inputs is presented in Fig. 12. The values of $|\rho| \geq 0.60$ with the cake solids content are found for the pressure difference Δp, air temperature at the vacuum pump inlet T_{vp}, the dewatering time t_{dw}, the air flow rate at the vacuum pump outlet Q_a, and the interaction feature $\Delta p t_{dw}$. Other features presented in the correlation map were also considered to have an impact on the filter cake solids content and were thus included in the analysis.

This is an original manuscript of an article published by Elsevier in Separation and Purification Technology on 15 September 2019, available online: https://doi.org/10.1016/j.seppur.2019.03.091.

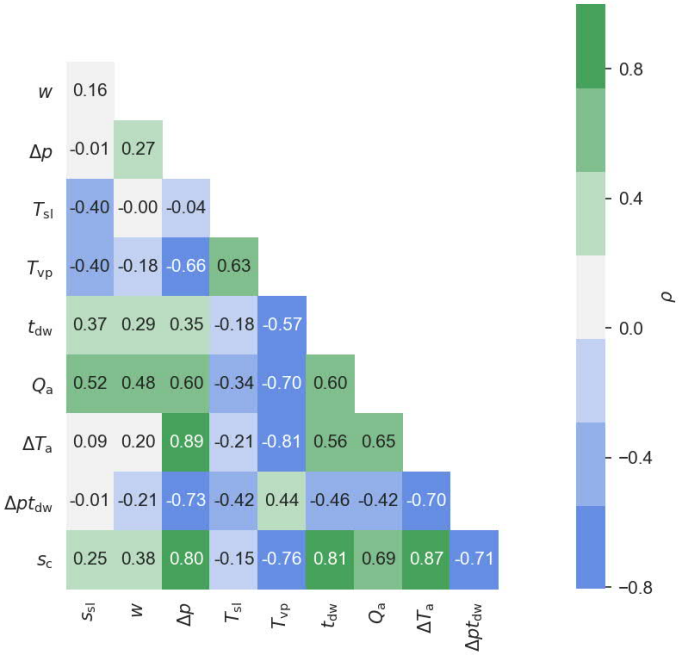

Fig. 12. Correlation map presenting the Pearson correlation coefficients ρ between the experiment settings, process variables, the two interaction features ΔT_a and Δpt_{dw}, and the filter cake solids content s_c.

The selection of features for the nine feature sets used as inputs to model the cake solids content was started from the bare minimum of Δp and w and increased and varied from set to set to see which features would be advantageous to the modeling and to keep the number of input features at a reasonable level. As these two features were the main controlled process variables in the experiments, they were included in each of the feature sets, in two of which Δp was included only in the interaction feature Δpt_{dw}.

Table 4. Features selected for different feature sets for experimentation as model inputs.

	Feature Set								
Features	**1**	**2**	**3**	**4**	**5**	**6**	**7**	**8**	**9**
s_{sl}						x	x	x	x
w	x	x	x	x	x	x	x	x	x
Δp	x	x	x			x	x	x	x
t_{dw}		x							x
T_{sl}									x
T_{vp}			x		x	x	x	x	x
Q_a					x	x	x	x	x
ΔT_a				x			x	x	x
Δpt_{dw}				x	x			x	x

For all other algorithms except Gradient Boosting, the selection between the dewatering time and the vacuum pump inlet air temperature favors the latter as can be seen in Fig. 13. This suggests that the temperature of air after passing through the filter cake would be a better indicator of the cake moisture content than the dewatering time. When relying on the two interaction features and the mass of solids deposited per unit area, regression results for all the other algorithms except for Gradient Boosting, again, take a turn to the worse. Selecting both the temperature and flow rate of air as inputs in addition to w and Δpt_{dw} helps all the algorithms to perform better.

For feature sets 6, 7, 8, and 9, which all also include the solids content of slurry and the pressure difference as inputs, the coefficients of determination R^2 for the ensemble decision tree algorithms Random Forest and Gradient Boosting rise to the 0.8 region. This indicates that these models are able to explain ~80 % of the variability in the cake solids content. The fact that the training and test scores for Random Forest are close to each other indicates a good fit of the algorithm for the non-linear regression problem. When including all the features as inputs, the linear regression algorithms Ridge and Elastic Net also achieve R^2 values above 0.7 and the Ridge mean absolute error (MAE) falls close to that of the Random Forest. The smallest MAE of 0.41 pp is achieved using the Gradient Boosting regression algorithm and the feature set seven with the R^2 values for training and testing of 0.86 and 0.82 respectively.

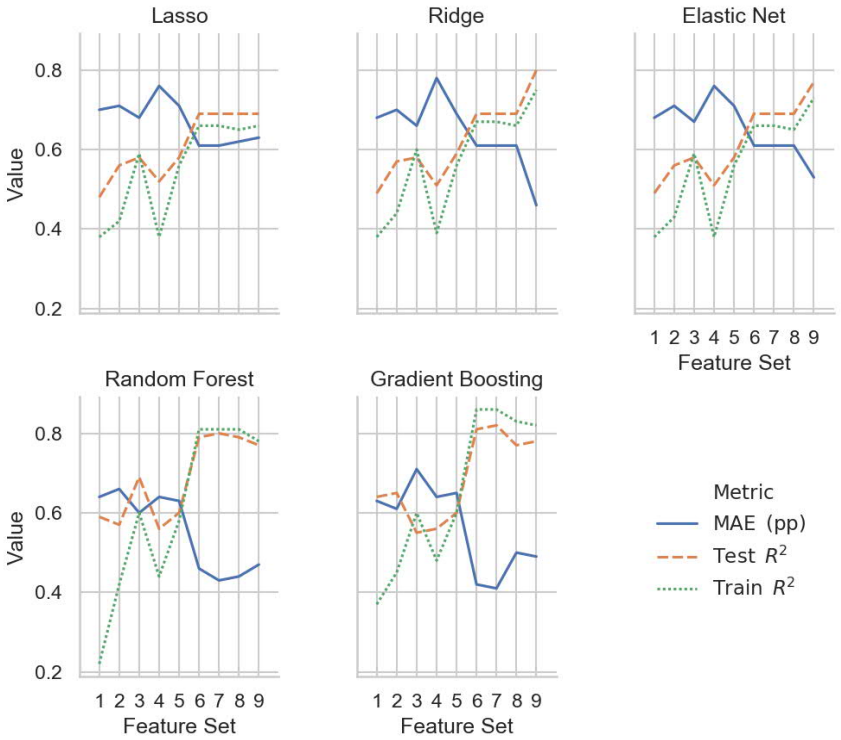

Fig. 13. Performance of the trained models for the filter cake solids content. The mean absolute error MAE is presented as percentage points of the target value. The coefficients of determination R^2 are presented both for the regression model training and testing.

Firstly, the application of the method on an industrial scale would require a proper instrumentation of the filter to measure the variables used as inputs for the model. Secondly, a sufficient number of

recordings of the input variables and an analysis of the corresponding cake samples at different operating points of the filter would be required to train the model. The solids content of the slurry as input variable could be replaced by a density measurement of the slurry.

5. Conclusions

The previously unexplored application of thermodynamics to cake vacuum filtration has proven highly beneficial for predicting the filter cake moisture content. The heat transfer between air forced through the filter cake, the water inside the filter cake, and the solids of the filter cake resulting from evaporation of water can be seen clearly from the results of this study. Predicting the cake solids content by using regression modeling with the vacuum pump inlet air temperature and the air flow rate as inputs in addition to the traditional vacuum filtration process variables makes it possible to explain 80% of the variance in the target variable by the model, while keeping the mean absolute error below 0.5 pp.

An interesting approach for predicting the filter cake moisture content would be the use of cake surface temperature as an input variable for modeling. The room temperature leak flow air mixes with the cooled air that has passed through the filter cake, warming the air/vapor mixture in the vacuum box especially at higher pressure differences with the increased leak flow. This moderates the cool down effect of evaporation in the vacuum box, which could be prevented by using the surface temperature of the filter cake as a key variable in the prediction. In addition to horizontal belt vacuum filters, the proposed method for real-time monitoring of the moisture content of the filter cake is applicable to other types of filters where similar temperature measurements can be made. However, the applicability of the method to air drying in pressure filters would require further investigation. Given the promising results of this pilot-scale research, next steps for future investigation of the technology could include a trial setup on an industrial scale. Another topic for future research could be the development of a rigorous mathematical model for evaporation using the governing equations for mass, momentum, and energy.

Regarding the energy consumption of vacuum filtration and the subsequent thermal drying of the calcite material investigated in this study, the following conclusions can be made:

1) The lowest total energy demand is achieved in the pressure difference range from 0.2 to 0.3 bar, when the cake is dewatered to approximately 84 wt.% solids content prior to thermal drying.
2) Finding the right combination of slurry solids content, mass of cake per unit area, and pressure difference is crucial in minimizing the specific energy consumption of vacuum filtration.

Lappeenranta University of Technology has patented the methods for the filter cake moisture estimation described in this publication.

Acknowledgements

The authors would like to thank Hanna Niemelä for providing language help during the writing process.

Funding: This work was supported by The Finnish Funding Agency for Technology and Innovation (Tekes).

References

[1] E.S. Tarleton, R.J. Wakeman, Institution of Chemical Engineers (Great Britain), Solid/liquid separation : equipment selection and process design, Butterworth-Heinemann, 2007.
[2] V. Karvonen, M. Huttunen, T. Kinnarinen, A. Häkkinen, Research focus and research trends in vacuum filtration – bibliographical analysis, Filtration. 18 (2018) 40–44.
[3] L. Besra, D.K. Sengupta, S.K. Roy, Particle characteristics and their influence on dewatering of kaolin, calcite and quartz suspensions, Int. J. Miner. Process. 59 (2000) 89–112. doi:10.1016/S0301-7516(99)00065-4.
[4] G. France, A. von Muralt, Horizontal vacuum belt filter control using on-line moisture analysis at Gregory coal mine, in: 11th Aust. Coal Prep. Conf. Exhib. Proc., 2007: pp. 82–93.
[5] H. Mao, F. Wang, F. Mao, Y. Chi, S. Lu, K. Cen, Measurement of water content and moisture distribution in sludge by ^{1}H nuclear magnetic resonance spectroscopy, Dry. Technol. 34 (2016) 267–274. doi:10.1080/07373937.2015.1047952.
[6] K. Phetpan, P. Sirisomboon, Evaluation of the moisture content of tapioca starch using near-infrared spectroscopy, J. Innov. Opt. Health Sci. 08 (2015) 1550014. doi:10.1142/S1793545815500145.
[7] T.J. Schmugge, T.J. Jackson, H.L. McKim, Survey of methods for soil moisture determination, Greenbelt, Maryland, 1979.
[8] R. Wakeman, The influence of particle properties on filtration, Sep. Purif. Technol. 58 (2007) 234–241. doi:10.1016/J.SEPPUR.2007.03.018.
[9] L. Svarovsky, Solid-liquid separation, 4th ed., Butterworth-Heinemann, 2000.
[10] S. Tarleton, R. Wakeman, Solid/Liquid Separation : Principles of Industrial Filtration., Elsevier Science, 2005.
[11] D.J. Condie, M. Hinkel, C.J. Veal, K. Boissy, D. Leclerc, Modeling the Vacuum Filtration of Fine Coal. III. Comparison of Models for Predicting Desaturation Kinetics, Sep. Sci. Technol. 35 (2000) 1467–1484. doi:10.1081/SS-100100236.
[12] A. Rushton, M. Hosseini, I. Hassan, The effects of velocity and concentration on filter cake resistance, in: Proc. Symp. Solid-Liquid Sep. Pract., Leeds, 1978: pp. 78–91.
[13] G.H. Hundy, A.R. Trott, T. Welch, Refrigeration, air conditioning and heat pumps, Fifth, Butterworth-Heinemann, Oxford, 2016.
[14] M.K. Das, P.P. Mukherjee, K. Muralidhar, Equations Governing Flow and Transport in Porous Media, in: Model. Transp. Phenom. Porous Media with Appl., Springer International Publishing, 2018: pp. 15–63. doi:10.1007/978-3-319-69866-3_2.
[15] I. Kovačević, M. Sourbron, The numerical model for direct evaporative cooler, Appl. Therm. Eng. 113 (2017) 8–19. doi:10.1016/J.APPLTHERMALENG.2016.11.025.
[16] I.C. Kemp, Fundamentals of Energy Analysis of Dryers, in: Mod. Dry. Technol. Vol. 4 Energy Savings, Wiley-VCH Verlag GmbH & Co. KGaA, Weinheim, Germany, 2012: pp. 1–45. doi:10.1002/9783527631681.ch1.
[17] J.R. Rumble, D.R. Lide, T.J. Bruno, CRC handbook of chemistry and physics, 99 th, CRC Press, 2018.

[18] L. Fortuna, S. Graziani, A. Rizzo, M.G. Xibilia, Soft Sensors for Monitoring and Control of Industrial Processes, Springer London, London, 2007. doi:10.1007/978-1-84628-480-9.
[19] B. Lin, B. Recke, J.K.H. Knudsen, S.B. Jørgensen, A systematic approach for soft sensor development, Comput. Chem. Eng. 31 (2007) 419–425. doi:10.1016/J.COMPCHEMENG.2006.05.030.
[20] P. Kadlec, B. Gabrys, S. Strandt, Data-driven Soft Sensors in the process industry, Comput. Chem. Eng. 33 (2009) 795–814. doi:10.1016/J.COMPCHEMENG.2008.12.012.
[21] P. Kadlec, R. Grbić, B. Gabrys, Review of adaptation mechanisms for data-driven soft sensors, Comput. Chem. Eng. 35 (2011) 1–24. doi:10.1016/J.COMPCHEMENG.2010.07.034.
[22] F.A.A. Souza, R. Araújo, J. Mendes, Review of soft sensor methods for regression applications, Chemom. Intell. Lab. Syst. 152 (2016) 69–79. doi:10.1016/J.CHEMOLAB.2015.12.011.
[23] Z. Ge, Review on data-driven modeling and monitoring for plant-wide industrial processes, Chemom. Intell. Lab. Syst. 171 (2017) 16–25. doi:10.1016/J.CHEMOLAB.2017.09.021.
[24] B. Bidar, J. Sadeghi, F. Shahraki, M.M. Khalilipour, Data-driven soft sensor approach for online quality prediction using state dependent parameter models, Chemom. Intell. Lab. Syst. 162 (2017) 130–141. doi:10.1016/J.CHEMOLAB.2017.01.004.
[25] L. Yao, Z. Ge, Variable selection for nonlinear soft sensor development with enhanced Binary Differential Evolution algorithm, Control Eng. Pract. 72 (2018) 68–82. doi:10.1016/J.CONENGPRAC.2017.11.007.
[26] E. Szymańska, Modern data science for analytical chemical data – A comprehensive review, Anal. Chim. Acta. 1028 (2018) 1–10. doi:10.1016/J.ACA.2018.05.038.
[27] Z. Ge, Z. Song, S.X. Ding, B. Huang, Data Mining and Analytics in the Process Industry: The Role of Machine Learning, IEEE Access. 5 (2017) 20590–20616. doi:10.1109/ACCESS.2017.2756872.
[28] M. Huttunen, L. Nygren, T. Kinnarinen, A. Häkkinen, T. Lindh, J. Ahola, V. Karvonen, Specific energy consumption of cake dewatering with vacuum filters, Miner. Eng. 100 (2017) 144–154. doi:10.1016/J.MINENG.2016.10.025.
[29] T. Kudra, E. Pallai, Z. Bartczaki, M. Peter, Drying of paste-like materials in screw-type spouted-bed and spin-flash dryers, Dry. Technol. 7 (1989) 583–597. doi:10.1080/07373938908916612.